Temperature Dependence of the Raman Spectrum and the Depolarization Spectrum of Amorphous As_2S_3†

R. J. Kobliska*‡ and S. A. Solin
The Department of Physics and The James Franck Institute, The University of Chicago, Chicago, Illinois 60637
(Received 26 January 1973)

The polarized Stokes and anti-Stokes Raman spectrum of amorphous As_2S_3 has been measured at several temperatures in the range 20–448 °K with a He-Ne laser, and at room temperature with a c.w. dye laser. Using the Shuker–Gammon data-reduction method, the approximate density of vibrational states has been determined from the Raman spectra and has been found to be temperature independent. A new type of spectrum, the depolarization spectrum, has been measured for amorphous As_2S_3. The depolarization spectrum has been defined to be the dispersion of the Raman depolarization ratio. The measured Raman and depolarization spectra have been used to test the validity of the two structural models of vitreous As_2S_3 proposed to date, namely: the planar-random-network model of Bermudez and the molecular model of Lucovsky and Martin. It has been shown that *both* models can be used to calculate Raman spectra in reasonable agreement with experiment while only the molecular model is compatible with the observed depolarization spectrum. Further, it has been demonstrated that the depolarization spectrum, not the Raman spectrum, provides a test of the applicability of the Shuker–Gammon data-reduction technique to a given amorphous solid. The low-temperature ($\sim$20 °K) Raman and room-temperature infrared transmission spectra of orpiment, the crystalline form of As_2S_3, have been measured. Several lines unresolved in previously reported room-temperature Raman spectra of orpiment have been resolved in the low-temperature spectra. The envelope of the approximate density of vibrational states of orpiment has been found to resemble remarkably the approximate density of vibrational states of amorphous As_2S_3. This resemblance has been explained using the molecular model.

I. INTRODUCTION

The current interest in the Raman spectra of amorphous solids is a manifestation of the relationship between the structure (i.e., range of order) and the vibrational spectra of disordered materials. Naturally, a considerable amount of research effort has been directed towards the fourfold coordinated semiconducting elements and compounds since those are the substances which are the most tractable from a theoretical point of view. For example, amorphous Si and Ge exhibit only translational disorder and no compositional disorder.[1] On the other hand, with the exception of the chalcopyrites, the fourfold coordinated amorphous semiconductors can only be prepared in the form of thin films.[2] But the electrical and optical properties as well as the structural properties of amorphous films are notoriously dependent upon the method of preparation and environmental history.[3] In fact, there is still some debate[4] over what constitutes a "truly" amorphous film notwithstanding the theoretical work of Galeener[5] and experimental measurements of the optical absorption edge of void-free amorphous Ge and Si films by Donovan *et al.*[6] and Fisher and Donovan,[7] respectively.

Fortunately, there is a class of disordered semiconducting solids, the bulk chalcogenide glasses, which are free from the experimental ambiguities attendant to thin films. In fact, the chalcogenide glasses can be prepared in film as well as bulk form. Most noteworthy of the chalcogenides is vitreous As_2S_3. This material has long been used in infrared lens and window applications and is thus commercially available in reproducible form.[8] In addition, vitreous As_2S_3 is transparent in the red region of the visible spectrum.[9] For these reasons we have chosen As_2S_3 as an ideal material with which to study the detailed temperature and polarization dependence of the spontaneous Raman spectrum of a bulk semiconducting amorphous solid.

The thermal, electrical, and optical properties of vitreous As_2S_3 have been extensively studied by many researchers.[10] It is, to date, the only amorphous solid in which the resonance Raman effect has been observed.[11] Ward, who first measured the spontaneous Raman spectra of this material,[12] reported structure which has since been shown by us to be absent from spectra recorded under proper experimental conditions.[13] More recently, Lucovsky has studied the infrared reflection spectra of amorphous As_2S_3.[14] Using the molecular model of Lucovsky and Martin,[15] he has calculated the dynamic effective charge of the optical modes and reconciled an oscillator fit to the reflectivity data with the polarized Raman results which we report here.

In contrast to the molecular model of Lucovsky and Martin, Bermudez has proposed a computer-generated two-dimensional A_2B_3 disordered-net-

work model for the structure of As_2S_3 and As_2Se_3.[16] From this model he, like Lucovsky, calculates properties of the Raman cross section which are in reasonable agreement with experiment. However, it is in the predicted polarization properties of the Raman spectrum that the molecular model and two-dimensional model show marked differences. We will show that the two-dimensional random-network model is not consistent with our polarized Raman spectra whereas the molecular model is remarkably accurate in this regard.

It is the polarization properties of the Raman spectra which provide the critical test of distinctly different structural models of amorphous As_2S_3 and not the frequency-shift dependence of the spontaneous Raman cross section. Therefore, plots of the Raman depolarization ratio as a function of frequency should provide valuable, if not primary, information on the structural features of amorphous solids. The attention given to polarization properties by those concerned with Raman scattering from amorphous solids has been underwhelming; invariably the polarization properties are merely reported as empirical observations[17] or are completely neglected.[18] This is particularly surprising since the spontaneous Raman cross section is not a physical property which is amenable to a universal interpretation consistent with all amorphous solids. For solids such as Si and Ge which are tetrahedrally bonded in both the amorphous and crystalline phase the spontaneous Raman cross section is believed to be intimately related, if not identical to, an appropriately smoothed density of vibrational states of the crystal.[17] On the other hand, no such connection exists between the density of vibrational states of orpiment, the crystalline form of As_2S_3, and the spontaneous Raman cross section of vitreous As_2S_3.[15] Nevertheless, we will show that the Raman spectrum of crystalline As_2S_3 can still yield valuable information about the vibrational properties of amorphous As_2S_3 and vice versa. Though the infrared and Raman spectra of orpiment have been thoroughly studied,[19,20] we have rerecorded both spectra in order to compare them, particularly the latter, with the corresponding spectra of vitreous As_2S_3 taken under identical experimental conditions. Incidental to these measurements we have been able to observe several new phonon lines in the low-temperature (~20 °K) Raman spectrum of orpiment which were unresolved in the previously reported room-temperature measurements.

Crystalline As_2S_3 exhibits a layered structure, the layers of which are composed of distorted but coupled pyramidal AsS_3 units.[21] The optical properties of the crystal are dominated by the two-dimensional layer symmetry and not by the three-dimensional space-group symmetry.[19,20] There is evidence that both the layer character as well as the pyramidal units exist in vitreous As_2S_3.[22] In addition, Rubenstein and Taylor[23] have interpreted the nuclear-quadrupole-resonance (NQR) spectrum of As^{75} in vitreous As_2S_3 as indicating a distribution in pyramidal apex bond angles with a maximum spread of ± 2° about the mean. Using the above information and our Raman-scattering results we are able to estimate the dispersion of the valence force constants of the molecular model.

II. EXPERIMENTAL

The samples of amorphous As_2S_3 used in this study were obtained from the Servo Corp. of America under the trade name Servofrax.[8] They were rectangular parallelepipeds of dimension 6×6×1 mm and were polished on all six surfaces to a flatness of $\frac{1}{2}\lambda$ measured at ~5000 Å. The samples were extremely homogeneous and optically isotropic; we measured a room-temperature extinction ratio of 30 dB for polarized He-Ne laser light at 6328 Å. Thus, our polarization studies are unencumbered by the undesirable effects of strain-induced birefringence. A large sample (typical dimension 1 in.) of Nevada orpiment used for the study of crystalline As_2S_3 was obtained from P. Moore of the Geophysical Sciences Dept. at the University of Chicago. From it a slab of single crystal 1 mm thick was cleaved and subsequently cut into several parallelepipeds of dimensions ~4×4×1 mm having faces in the *ac* crystal plane (see Sec. III B for a discussion of the crystal symmetry).

All of the Raman spectra reported in this paper were recorded using the right-angle scattering geometry. Most of the spectra were excited with 50 mW of 6238-Å He-Ne laser radiation[24]; however, we also report spectra excited by an argon-ion laser[25] and by a cw dye laser[24] operating, respectively, at 5145 and 5910 Å. The Raman-scattered radiation was dispersed by a Jarrel–Ash model 25-100 double monochromator[26] and detected by an ITT model FW 130 phototube[27] coupled to a photon counting system. Peak signals of ~300 counts/sec were obtained from vitreous As_2S_3 with a spectral slit width of 5.4 cm^{-1} and a dark count of 1.3 counts/sec.

For low-temperature measurements, a five-window Andonian throttling cryostat[28] was used, while for high-temperature measurements a three-window home-made optical oven was employed. In both devices, the sample was immersed in a bath of He gas which was maintained at the desired measurement temperature. Below 150 °K a carbon thermometer and bridge-type controller were used to measure the sample temperature to within ± 0.1 °K and maintain it constant to within ± 0.01 °K. A copper-constantin thermocouple was used to measure sample temperatures in the range 150–448 °K

but no automatic controller was used for that temperature interval. Therefore, reported sample temperatures between 150–448 °K have an estimated error of ± 4 °K.

Vitreous As_2S_3 is ostensibly transparent at 6238 Å; its absorption coefficient at that wavelength and at 300 °K is ~0.8 cm^{-1}.[9] However, the small residual absorption coupled with the very low thermal conductivity of this substance (4×10^{-4} cal/ sec cm °C)][10] caused severe optical damage to samples which were exposed to as little as 50 mW of He-Ne laser radiation focused to yield an estimated power density of only 2 kW/cm^2. Even when immersed in superfluid He, samples of vitreous As_2S_3 suffered subsurface damage upon exposure to 2 kW/cm^2 of 6328-Å radiation! Similarly, at liquid-nitrogen temperature crystalline As_2S_3 exhibits negligible absorption at a photon energy of 2.41 eV(5145 Å),[9] yet when immersed in superfluid He this material could tolerate less than 80 kW/cm^2 of green argon laser radiation.

It is interesting to note that the damage to vitreous As_2S_3 occurred instantaneously as evidenced by the absence of any Raman signal when the incident He-Ne laser-power density exceeded 2 kW/cm^2. However, when excited with 5145-Å radiation having a power density in excess of 80 kW/cm^2, the Raman spectrum of crystalline As_2S_3 exhibits a gradual decrease in intensity with increasing exposure time. Both crystalline and amorphous As_2S_3 undergo a color change in the irradiated region; the former transforms from yellow to red, the latter from red to black. Light- and heat-induced color changes have previously been observed in amorphous As_2S_3[29] although to our knowledge no other measurements of this effect have been made at liquid-helium temperature. Apparently the very properties of amorphous As_2S_3 which make it a choice material for storing optical information[30] are detrimental to the observation of its Raman spectrum. We were able to obtain reproducible Raman spectra from amorphous and crystalline As_2S_3 simply by defocusing the incident laser beam to obtain a 3-mm spot size (at the $1/e^2$ power points for the TEM_{00} mode) at the sample.[11]

Each of the Raman spectra reported here has been computer corrected for the dispersion and polarization dependence of the instrumental transfer function $\tau(\omega_s)$, ω_s being the frequency of the Raman-scattered photon.[31] Two Raman polarization configurations have been employed and are denoted by VV and HV. I_{VV} is the scattered intensity when both incident and scattered radiation are polarized perpendicular to the scattering plane, i.e., vertical in the laboratory coordinate system, while I_{HV} is the scattered intensity when the incident radiation is polarized in the scattering plane and the scattered radiation is polarized perpendicular to the scattering plane. The depolarization ratio ρ is given by $\rho = I_{HV}/I_{VV}$. Note that for the polarization configurations discussed above, the scattered radiation is always polarized perpendicular to the scattering plane. Therefore, depolarization ratios can be calculated directly from the raw Raman data without correcting for the instrumental transfer function.

Measurements of the unpolarized infrared transmission spectra of orpiment in the range 150–600 cm^{-1} were made with a Perkin–Elmer model 180 spectrophotometer[32] operating in the constant-I_0 (dual-beam) mode. The cleavage properties of orpiment preclude infrared reflection or transmission measurements in which the incident radiation propagates parallel to the layers. Therefore in the hope of examining infrared modes active along the b axis of the crystal a "mull" sample of powdered crystalline As_2S_3 was examined. The techniques for preparing mull samples are well known[33] and need not be elaborated upon here except to note that "nujol" oil was used as the suspending medium.

III. RESULTS AND DISCUSSION

A. Approximate Density of Vibrational States

Shuker and Gammon[34] have suggested a data-reduction technique which enables one to derive from the first-order Raman spectrum of an amorphous solid what we call an "approximate" density of states. Specifically, the Raman intensity is obtained from the Fourier transform of the space-time correlation function of the fluctuations in the dielectric constant of the material. The Stokes Raman intensity is given by

$$I_{\alpha\beta,\gamma\delta}(\omega, T) = \sum_b C_b^{\alpha\beta,\gamma\delta}\left(\frac{1}{\omega}\right)[1+n(\omega, T)]g_b(\omega), \quad (1)$$

where $I_{\alpha\beta,\gamma\delta}(\omega, T)$ is the intensity at a frequency shift ω, $g_b(\omega)$ is the density of vibrational energy states in band b, $n(\omega, T)$ is the Bose–Einstein occupation number for a phonon of frequency ω at equilibrium temperature T, $C_b^{\alpha\beta,\gamma\delta}$ are polarization-dependent coupling coefficients that contain the coupling of band b to the optical radiation field, and $\alpha\beta(\gamma\delta)$ index the incident (scattered) -light polarization. It is assumed in Eq. (1) that all vibrations within a band couple equally to the radiation. The anti-Stokes Raman intensity is obtained simply by replacing $[n(\omega, T)+1]$ by $n(\omega, T)$ in Eq. (1). If the coupling coefficients are band independent, the approximate density of states

$$g_A(\omega) = \sum_b g_b(\omega) \quad (2)$$

is proportional to the observed Stokes Raman intensity divided at each frequency shift ω by $[n(\omega, T)+1]/\omega$ [or $n(\omega, T)/\omega$ for the anti-Stokes intensity].

Equation (1) predicts a continuum first-order spectrum for an amorphous solid in contrast to the discrete-line Raman spectrum exhibited by crystalline solids. The discrete-line character of the first-order Raman spectrum of a crystal is a direct consequence of wave-vector (or crystal momentum) conservation[35]; only the zone-center ($\vec{k}\sim 0$) phonons can participate in the scattering process. But the wave vector does not represent a "good" quantum number for an amorphous solid since such a solid possesses no long-range order. Therefore, *all* vibrational modes can participate in the scattering process and the resultant continuous spectrum is, assuming band-independent coupling coefficients, proportional to the total density of vibrational states. For essentially the same reasons, the infrared spectrum of an amorphous solid is, assuming band-independent coupling coefficients (i.e., constant matrix elements), also proportional to the approximate density of vibrational states.

The Raman intensity calculated from Eq. (1) is a function of only the phonon frequency and absolute temperature. The well known ω_s^4 dependence of an induced-dipole scatterer[35] is contained in the coupling coefficients and is apparently assumed by Shuker and Gammon to be constant over the range of Raman-scattered photon frequencies, i.e., 5–380 cm^{-1} for vitreous As_2S_3. However, for spectra excited by the 6328-Å radiation of a He-Ne laser, the ω_s^4 term for a 5-cm^{-1} Stokes shift is 9% larger than the corresponding term for a 380-cm^{-1} Stokes shift. Therefore we correct our Raman data for both the instrumental transfer function and the ω_s^4 term and obtain from Eq. (1) and the Stokes spectrum an approximate density of states given by

$$g_A(\omega)=\left(\tau_{\parallel}(\omega_i-\omega)\,\frac{1}{\omega}\,(\omega_i-\omega)^4[n(\omega,T)+1]\right)^{-1} \times\begin{cases} I_{VV}(\omega,T)/C^{VV} \\ I_{HV}(\omega,T)/C^{HV} \end{cases}. \quad (3)$$

Here $\tau_{\parallel}(\omega_i-\omega)$ is the instrumental transfer function for light polarized parallel to the spectrometer grating grooves, ω_i is the frequency of the incident photon, and

$$\omega_s=\omega_i-\omega. \quad (4)$$

The approximate density of states can also be determined from the anti-Stokes spectra by making the following transformations in Eq. (3):

$$\omega_i-\omega\rightarrow\omega_i+\omega$$
and
$$[n(\omega,T)+1]\rightarrow n(\omega,T). \quad (5)$$

In principle, the Raman data should also be corrected for the temperature dependence and dispersion of the absorption coefficient and reflectivity

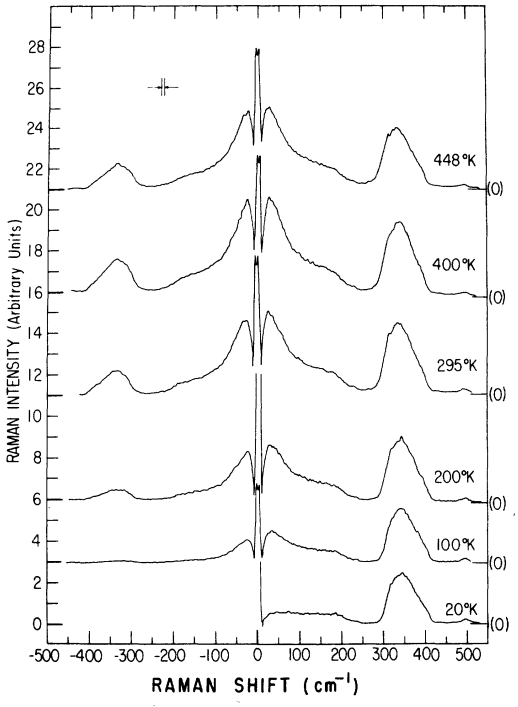

FIG. 1. Temperature dependence of the computer-smoothed right-angle Raman spectrum of vitreous As_2S_3. The incident light was polarized perpendicular to the scattering plane and no analyzer was used in the collection optics. The region $|\Delta\nu|\leq 11$ cm^{-1} has been artificially treated by the computer and should be ignored. The spectra were recorded with a spectral slit width of 5.4 cm^{-1}. The (0)'s at the right of the figure indicate the baselines of the corresponding spectra. These spectra were excited with the 6328-Å radiation from a He-Ne laser.

at the frequencies of the incident and scattered photons. These corrections are crucial to the observation of the resonance Raman effect[11] but have been omitted here since they require extensive computer calculation and introduce no alteration into our interpretation of the Raman data presented below.

Figure 1 shows the temperature dependence of the computer-smoothed[36] polarization-unanalyzed Stokes and anti-Stokes Raman spectrum of vitreous As_2S_3. The quasicontinuous character of the spectra and the highly temperature-dependent low-energy peak at ~ 30 cm^{-1} are typical of spontaneous first-order Raman scattering from an amorphous solid.[37] We note that at any given frequency shift in the anti-Stokes region the Raman intensity is linearly proportional to the Bose–Einstein occupation number, $n(\omega, T)$; thus, we are indeed observing a first-order Raman effect. In order to further verify that the structure in the Raman spectra of vitreous As_2S_3 at 140, 189, 230, and 490 cm^{-1} reported by Ward[12] was in fact absent from our spectra they were excited with the 5910-Å radiation

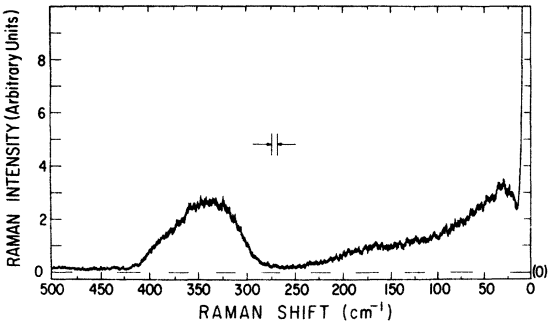

FIG. 2. Room-temperature right-angle Stokes–Raman spectrum of vitreous As_2S_3 excited by the 5910-Å radiation of a cw dye laser. Approximately 15 mW of laser radiation was incident on the sample and no analyzing polarizer was used. This spectrum was also recorded with a spectral slit width of 5.4 cm^{-1}. The abscissa is linear in wavelength rather than wave number.

from a cw dye laser.[24] The result is shown in Fig. 2. We also used the 5145-Å argon laser line and the reflection scattering geometry to record the Raman spectrum of vitreous As_2S_3. However, as a result of the high-absorption coefficient at 5145 Å and low thermal conductivity the threshold laser power for damaging the sample was so low that definitive spectra could not be obtained.

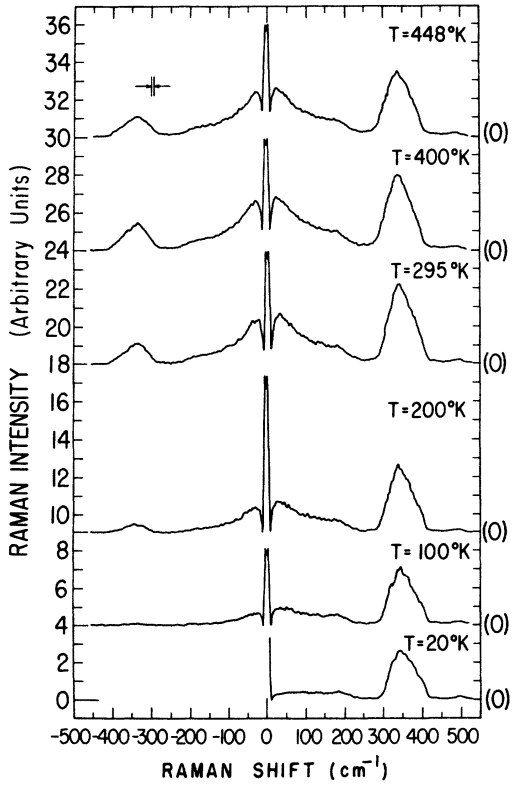

FIG. 3. Computer-smoothed VV-polarized Raman spectra recorded at the temperatures indicated.

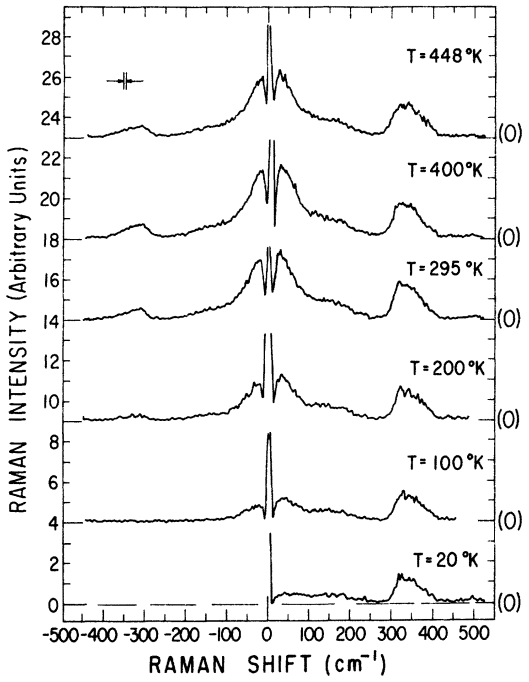

FIG. 4. Computer-smoothed HV-polarized Raman spectra recorded at the temperatures indicated.

In Figs. 3 and 4 we have shown, respectively, the computer-smoothed transfer-function-corrected VV- and HV-polarized Raman spectra of amorphous As_2S_3. As can be seen, for each measurement temperature the ratio of the intensities of the Raman peaks at ~ 30 and 344 cm^{-1} is quite different for the two polarizations; the low-energy vibrations are more pronounced in the HV spectrum. Thus, for vitreous As_2S_3 the coupling coefficients in Eq. (1) are clearly *not* band independent. It is for this reason that we label the density of states deduced from the theory of Shuker and Gammon an approximate density of states.

Figures 5 and 6 show the approximate densities of states derived by applying, in the manner described above, the expression given on the right-hand side of Eq. (3) to the VV and HV Raman spectra of Figs. 3 and 4, respectively. The anti-Stokes spectra of Figs. 5 and 6 exhibit a much lower signal-to-noise ratio than the corresponding Stokes spectra; therefore, the anti-Stokes–derived approximate densities of states exhibit a poor signal-to-noise ratio, especially at low temperature. The approximate densities of states deduced from the HV and VV Raman spectra of vitreous As_2S_3 are, disregarding corrections for absorption, identical but for the following three exceptions:

(i) The inner peak at ~ 180 cm^{-1} when compared to the peak at 344 cm^{-1} is more intense in the approximate density of states derived from the HV Raman spectra than from the VV spectra. This

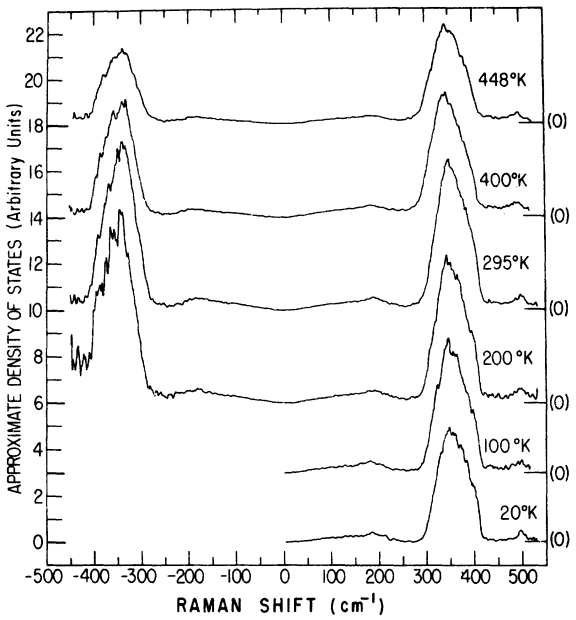

FIG. 5. Temperature dependence of the approximate density of vibrational states of amorphous As_2S_3 deduced from the Stokes and anti-Stokes VV-polarized Raman spectra of Fig. 3.

again is a manifestation of the band *dependence* of the coupling coefficients in Eq. (1).

(ii) The inner peak occurs at a slightly lower frequency shift in the HV-derived approximate density of states compared to its position in the VV-derived approximate density of states.

(iii) The high-energy peak shifts from 344 cm^{-1} in the VV-derived approximate density of states to 325 cm^{-1} in the HV-derived approximate density of states.

In support of the Shuker–Gammon theory, we note that the approximate densities of states shown in Figs. 5 and 6 are temperature independent. One expects a true density of vibrational states of an amorphous solid to change very little with temperature over the range of temperatures explored in this paper.

It is interesting to note that the Shuker–Gammon theory was developed to explain the Raman spectra of molecular-type glasses, e.g., vitreous quartz, and vitreous As_2S_3, yet it is for these materials that the theory is *least* successful as far as the assumption of band independence of the coupling coefficients $C_b^{\alpha\beta,\gamma\delta}$ is concerned. Moreover, the approximate densities of states deduced from the Raman and infrared spectra of glassy amorphous solids are not identical.[14,15] Ironically, it is the tetrahedrally bonded thin-film amorphous solids such as Ge and Si that are most compatible with the Shuker–Gammon theory. For instance, consistent with the assumption of band-independent coupling coefficients, the VH- and HH-polarized Raman spectra of amorphous Si are, to within a constant scale factor, essentially identical[17] while the approximate densities of states deduced from both Raman and infrared measurements are similar.[17,38]

B. Spectra of the Crystal

Crystalline As_2S_3 which has C_{2h}^5 space-group symmetry possesses a micaceous layered structure.[21] Zallen *et al.*[19] and Mathieu and Poulet[20] have found that it is the C_{2v} layer symmetry and not the three-dimensional space-group symmetry which determines the optical properties of the crystal. We have measured the Raman spectrum of crystalline As_2S_3 using the right-angle scattering geometry with the exciting radiation incident along the crystal *b* axis, i.e., perpendicular to the layers and with unknown orientation in the *ac* plane. The spectra were recorded at room temperature and at 20 °K using 6328- and 5145-Å laser excitation lines, respectively. The low-temperature spectrum shown in Fig. 7 contains lines at 315 and 360 cm^{-1} which were barely resolved in our room-temperature measurements. Weak low-frequency Raman lines such as the one reported at 36 cm^{-1} exhibit a marked decrease in intensity with decreasing temperature; they are not present in Fig.

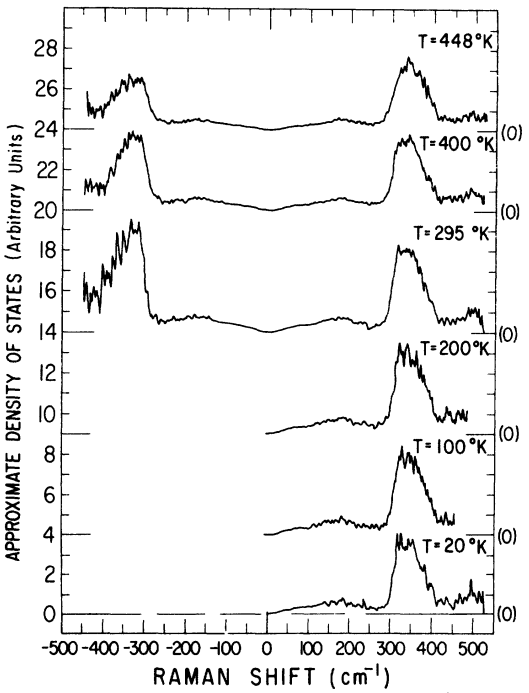

FIG. 6. Temperature dependence of the approximate density of vibrational states of amorphous As_2S_3 derived from the Stokes and anti-Stokes HV-polarized Raman spectra of Fig. 4.

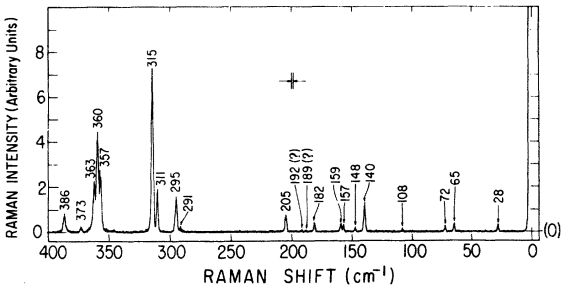

FIG. 7. Raman spectrum of crystalline As_2S_3 recorded at 20 °K using the 5145-Å line of an argon-ion laser.

7, but have been observed in our room-temperature measurements [see Table I].

Zallen *et al.*[19] examined only single crystals of As_2S_3. They could not observe vibrations belonging to the B_2 irreducible representation of the C_{2v} point group since such vibrations are infrared active only for light polarized parallel to the b axis of the crystal. However, Mathieu and Poulet[20] studied the infrared transmission of both mull (powdered) samples and single crystals. They concluded that three modes at 179, ~ 290, and 394 cm^{-1}, which were definitely present in the spectra of the mull samples but absent from the spectra of the single crystal, have B_2 symmetry. We have also measured the infrared transmission spectrum of a mull sample of crystalline As_2S_3 and of a thin single crystal. The results of these measurements, both of which were made using unpolarized light, are shown in Fig. 8. In Table I we summarize our Raman and infrared measurements of crystalline As_2S_3 and compare them with the results obtained by Mathieu and Poulet[20] and by Zallen *et al.*[19]

C. Comparison of the Raman Spectra of Crystalline and Amorphous Phases

Local structural similarities in the amorphous and crystalline phases of a given substance should

TABLE I. Frequencies and symmetries of the optical phonons of orpiment determined from the present room-temperature Raman and infrared measurements (frequencies only) and the previous measurements of Mathieu and Poulet (Ref. 20) and Zallen *et al.* (Ref. 19).

Raman shift in cm^{-1}			ir frequency in cm^{-1}			Symmetry assignment[a]	
Authors	Zallen *et al.*	Mathieu and Poulet	Authors	Zallen *et al.*	Mathieu and Poulet	Zallen *et al.*	Mathieu and Poulet
26	25	25					B_2?
37	36	35					A_2?
					52		A_1
63	63	60					?
67[b]					67		A_1
70	69	69					?
106	107	105					A_2
136	136	134		140		A_1	B_2?
					139		A_1
144[b]							
154	154	152	155	159	150	A_1	A_1
157		156			158		A_1
179	179	179	179	181	176	B_1	B_2
					182		B_1
203	204	201	199	198	201	A_1	A_1
			212[b]				
			244	244		B_1	
			278	279		B_1	
290		290					B_2+A_2
294	293						
		300	300	299	300	B_1	B_1
309	311	309	311	311	310	A_1	A_1
312[b]							
324	326						
			346	345	346	B_1	B_1
354	355	355	353	354	354	A_1	A_1
356[b]							
360	359	359	362		361		A_1
368		364					A_2
				375		B_1	
383	382	381	382	383	380	A_1	B_1
			392		394		B_2

[a]The symmetry convention is that of Ref. 20.

[b]Previously unreported.

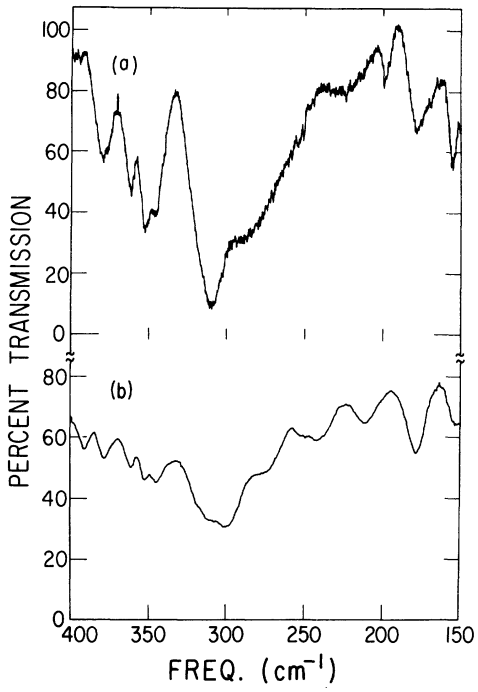

FIG. 8. (a) Infrared transmission spectrum of a partially unoriented single crystal of orpiment. The radiation was incident along the crystal b axis. (b) The infrared transmission spectrum of a mull sample of orpiment.

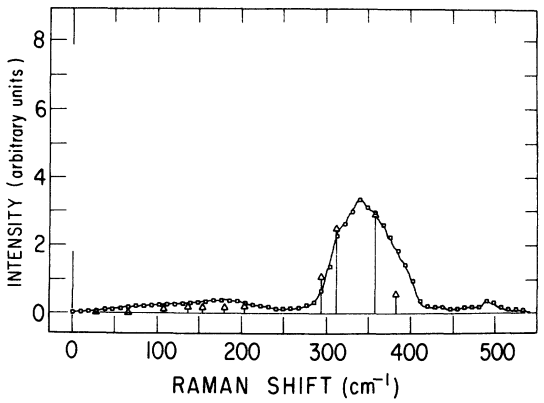

FIG. 9. Comparison of the approximate densities of vibrational states of amorphous and crystalline As_2S_3 normalized at 355 cm^{-1}. The data were derived from the polarization-unanalyzed Raman spectra of the amorphous and crystalline phases using Eq. (3) of the text with $\tau_{\parallel}(\omega_i - \omega) = \text{constant}$ and $I(\omega, 300\ °K)_{\text{unpolarized}}$ in the right-hand bracket.

be reflected in the optical spectra of the two phases. Therefore we have recorded the room-temperature polarization-unanalyzed Raman spectra of amorphous and crystalline As_2S_3, under *identical* experimental conditions. The peak intensities of the prominent lines in the spectrum of orpiment have been used in Eq. (3) to determine an approximate density of crystalline states at the discrete eigenfrequencies of the Raman-active vibrations. The approximate densities of states for crystalline and amorphous As_2S_3 have been normalized to the 355-cm^{-1} peak of the crystal and are plotted in Fig. 9.[39] The similarity between the two sets of data is remarkable; the approximate density of states for the amorphous phase is, but for minor discrepancies, the envelope of the corresponding crystal data points. The comparison is at best qualitative since the dependence of phonon intensities on crystal orientation has not been considered. It might be argued that the Raman spectrum of powdered (crystalline) As_2S_3 would be more appropriate for comparison to the spectrum of the amorphous phase. However, we could not have studied the powder under identical experimental conditions as used for the amorphous phase. Moreover, the envelope of the polarization-unanalyzed Raman lines of the crystal was relatively insensitive to sample orientation.

D. Depolarization Spectrum

The polarization properties of the Raman spectrum of a crystalline material can be used to determine the group-theoretical symmetries of the vibrational eigenstates. If oriented single crystals are studied it is possible, using modern-day techniques,[40] to determine the structure, i.e., the zero and nonzero components, of the Raman tensor of each active mode and therefore its symmetry species.

It is not possible, however, to determine the structure of the Raman tensor from the spectrum of a polycrystalline solid or powdered crystalline material, or a liquid or gas because the crystallites or molecules, respectively, are randomly oriented in space. Instead, the symmetry property of each line in the Raman spectra of such substances is quantitatively characterized by a depolarization ratio ρ defined as the ratio of the intensity of scattered light polarized in the scattering plane to that polarized perpendicular to the plane.[41] Polycrystals, powders, liquids, gases, and single crystals all exhibit discrete first-order Raman spectra.[42] Therefore, the frequency dependence of the depolarization ratio of these substances[43] can be written in the general form

$$\rho(\omega) = \sum_{i=1}^{N} \rho_i \, \delta(\omega - \omega_i) \, . \tag{6}$$

Here we assume that no accidental degeneracies occur in the Raman spectrum which is composed of N discrete lines having zero width. Also, ρ_i is the depolarization ratio of the Raman line having frequency shift ω_i. The range of values which the depolarization ratio can assume will depend upon

TABLE II. The allowed values of the depolarization ratios ρ_i for linearly polarized incident radiation.

Material[a]	Vibrational mode type	Trace of Raman tensor	Range of ρ_i
Single crystal	Symmetric	$\neq 0$	$0 \leq \rho_i \leq \infty$
	Antisymmetric	$=0$	$0 \leq \rho_i \leq \infty$
	Doubly degenerate	$=0$	$0 \leq \rho_i \leq \infty$
	Triply degenerate	$=0$	$0 \leq \rho_i \leq \infty$
Polycrystal, Powdered crystal, Liquid, Gas	Symmetric	$\neq 0$	$0 \leq \rho_i < \frac{3}{4}$
	Antisymmetric	$=0$	$\rho_i = \frac{3}{4}$
	Doubly degenerate	$=0$	$\rho_i = \frac{3}{4}$
	Triply degenerate	$=0$	$\rho_i = \frac{3}{4}$

[a]Note: For disordered substances, i.e., gases, etc., Raman lines for which $\rho = \frac{3}{4}$ are characterized as depolarized while those having $\rho < \frac{3}{4}$ are polarized.

the type of Raman-active vibration to which it corresponds, the form of the material being examined, and the polarization properties of the exciting radiation. For linearly polarized exciting radiation, ρ_i can take on the values given in Table II.

Since the first-order Raman spectrum of an amorphous solid is continuous, the depolarization ratio associated with it is a continuous function of frequency shift. We can expect the structural features of the "depolarization spectrum" of an amorphous solid to reflect the different symmetry properties of the vibrational modes. (We will elaborate on this point in Sec. IV.) Moreover, by analogy with liquids and gases which are, of course, disordered systems, the "depolarization spectrum" of an amorphous solid has an amplitude bounded by the values 0 and $\frac{3}{4}$. In Fig. 10 is shown the depolarization spectrum of vitreous As_2S_3. This spectrum was calculated for each observation temperature T from the smoothed polarized Raman spectra $I_{HV}(\omega, T)$ and $I_{VV}(\omega, T)$ using

$$\rho(\omega) = I_{HV}(\omega, T)/I_{VV}(\omega, T) \qquad (7)$$

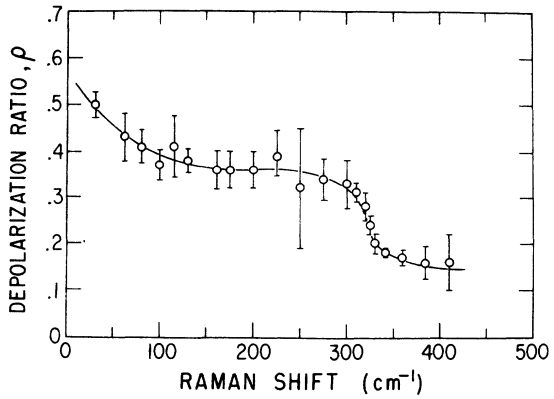

FIG. 10. Depolarization spectrum $\rho(\omega)$ of vitreous As_2S_3. Here $\rho(\omega) = \langle I_{HV}(\omega, T)/I_{VV}(\omega, T)\rangle_\omega$; the brackets indicate an average over all temperatures. The error bars indicate one standard deviation about the mean.

and was found to be temperature independent. The most noteworthy features of the spectrum are the sharp drop in depolarization ratio at ~ 315 cm^{-1}, the plateau between 100 and 300 cm^{-1}, and the rise to higher values with decreasing frequency shift below 100 cm^{-1}.

IV. STRUCTURAL MODELS AND OPTICAL SPECTRA

Two structural models of vitreous As_2S_3 now exist in the literature. Both models involve severe approximations yet each stresses a different aspect of the known structural features of vitreous As_2S_3.

A. Planar-Random-Network Model

Bermudez has extrapolated from the layer character[22] of both crystalline and vitreous As_2S_3 to a two-dimensional computer-generated disordered-network model of the amorphous phase.[16] A portion of the network is shown in Fig. 11(a). Note that the distribution in As-S-As bond angles is Gaussian while the S-As-S angle is fixed at 120°. Using his structural model and a two-parameter potential function involving nearest-neighbor central and noncentral interactions, Bermudez has generated and solved the equations of motion and has calculated the density of vibrational states of vitreous As_2S_3. His calculated density of states is compared in Fig. 12 to our measured approximate density of states. Suffice it to say that the agree-

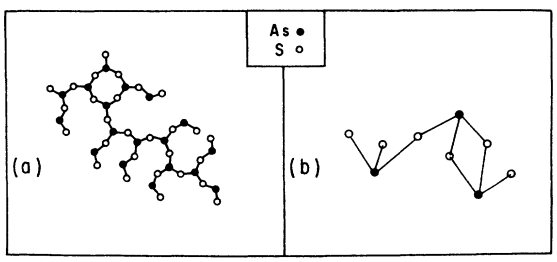

FIG. 11. Schematic representation of the atomic arrangements in (a) the planar-random-network model and (b) the molecular model.

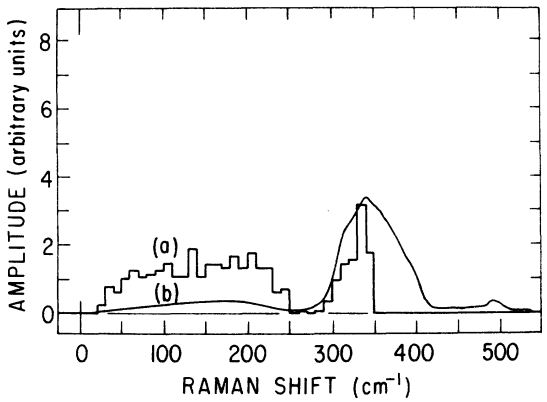

FIG. 12. Comparison between (a) the density of vibrational states calculated by Bermudez (Ref. 16) from the planar-random-network model of vitreous As_2S_3 and (b) the observed approximate density of states. The two curves have been normalized at 335 cm^{-1}.

ment is reasonable. The low-frequency continuum in the calculated density of states has been ascribed to bond-bending modes[16] whereas the peak at ~340 cm^{-1} corresponds to an antisymmetric As-S-As stretching vibration. The shoulder at 310 cm^{-1} derives from the stretching of the S-As-S bonds in the AsS_3 triangular units of which the network is composed.

If the network model accurately describes the dynamical motion in vitreous As_2S_3, then the eigenvectors calculated from that model for any specified eigenfrequency should yield depolarization values consistent with our measured depolarization ratio. Bermudez has analyzed his network model in terms of the internal modes of the AsS_3 *plane*-triangular unit and the As-S-As "water molecules." We therefore use those *local* structural units to determine the symmetries and depolarization ratios of the vibrational modes of amorphous As_2S_3.

The bending modes of the plane-triangular AsS_3 unit of the As-S-As "water molecule" can be either symmetric or antisymmetric. In fact, the low-energy continuum in the Raman spectrum of vitreous As_2S_3 (see Fig. 12) can result from an admixture of such modes and produce a depolarization spectrum with depolarization ratio $\rho(\omega) \leq \frac{3}{4}$. The results for the low-frequency regime shown in Fig. 10 neither conflict with nor confirm the predictions of the disordered-layer model. Consider now the high-frequency ($\omega > 250$ cm^{-1}) regime. Modes in the vicinity of the 340-cm^{-1} peak in the Raman spectrum have been assigned[16] to antisymmetric stretching deformations of the As-S-As "water molecule." The antisymmetric modes of a "water molecule," which has local point-group symmetry C_{2v}[44], give rise to depolarized Raman lines. From this and Table II we conclude that the depolarization ratio should be close to its maximum value of $\frac{3}{4}$ for $\omega \sim 340$ cm^{-1}. In addition the modes having eigenfrequencies ~310 cm^{-1} result, according to Bermudez, from a deformation of the AsS_3 planar unit. The eigenvectors corresponding to $\omega \sim 310$ cm^{-1} [see Fig. 5(f) of Ref. 16] represent a symmetric stretch of the AsS_3 unit which has local point-group symmetry D_{3h}.[44] But the in-plane symmetric-stretch vibrations of planar molecules with D_{3h} symmetry are totally symmetric[44] and as can be seen from Table II generate polarized Raman lines; i.e., $\rho < \frac{3}{4}$. Thus, the planar-disordered-network model predicts a rise in the depolarization spectrum between 310 and 340 cm^{-1} indicating a change from predominantly polarized to predominantly depolarized Raman scattering. This behavior, as can be seen from Fig. 10, is clearly inconsistent with the measured depolarization spectrum which shows a change from predominantly depolarized to prominently polarized scattering over the range 310–340 cm^{-1}.

B. Molecular Model

Lucovsky and Martin have proposed a molecular model based on the local atomic arrangement shown in Fig. 11(b) to explain the optical spectra of amorphous As_2S_3. They associate bands in the Raman and infrared spectra of vitreous As_2S_3 with the intramolecular and intermolecular vibrations of a basic structural unit, the AsS_3 pyramid. The intermolecular modes are identified with deformations of the triatomic bent chain As-S-As "water molecule." (In this respect the planar-random-network model and molecular model are quite similar.) The intermolecular coupling is presumed to be sufficiently weak that the pyramidal AsS_3 modes and the bridging chain As-S-As modes can be treated independently. In addition, from a group-theoretical point of view, the AsS_3 and As-S-As units are pyramidal XY_3 and bent planar X_2Y molecules with point-group symmetries C_{3v} and C_{2v}, respectively. The symmetry properties of such molecules have long been known and are discussed in detail by Herzberg.[44]

In Table III the symmetry species of the fundamental vibrations of the AsS_3 and As-S-As units are listed and the corresponding eigenfrequencies, calculated by Lucovsky and Martin from the molecular model, are compared with the positions of prominent features in the optical spectra of vitreous As_2S_3. Though features attributable to the As-S-As modes have not yet been observed in the optical spectra of amorphous As_2S_3,[46] the agreement between theory and experiment is quite respectable.

Observe from Table III that the 309-cm^{-1} ν_1 and the 344-cm^{-1} ν_3 modes are the symmetric (singlet) and antisymmetric (doubly degenerate) pyramidal

TABLE III. Symmetry properties and frequencies of the fundamental modes of vitreous As_2S_3 deduced from the molecular model.

Molecular structure and point-group symmetry	Mode[a]	Calculated frequency (cm^{-1})	Reported frequency (cm^{-1})	Symmetry species
	ν_1	344	344[b]	A_1
AsS_3 pyramid	ν_2	162	164[c]	A_1
∠ S-As-S = 97.2°	ν_3	310	310[c]	E
Point Group C_{3v}	ν_4	133	120–270[c]	E
As_2S "water molecule"	ν_1'	218	···	A_1
∠ As-S-As = 150°	ν_2'	55	···	A_1
Point group C_{2v}	ν_3'	438	···	B_1

[a]Modes are labeled according to Ref. 44. [b]References 12 and 13. [c]Reference 45.

deformations which generate, respectively, polarized and depolarized Raman lines. Each of these modes is broadened by the dispersion of the force constants and apex angles of the pyramidal units from which the amorphous phase is constructed. Therefore, the molecular model predicts correctly the change from predominantly depolarized scattering at 309 cm^{-1} to predominantly polarized scattering at 344 cm^{-1} shown in the depolarization spectrum of Fig. 10.

Pyramidal XY_3 molecules are somewhat unusual spectroscopically in that all of the polar modes of this structure are Raman active while all of the Raman active modes are polar.[47] The dominant ir active mode ν_3 has maximum intensity in the HV Raman spectrum; the dominant Raman-active mode ν_1 has maximum intensity in the VV Raman spectrum. Thus, the molecular model properly accounts for the shift in the high-frequency peak from 344 cm^{-1} in the VV-derived approximate density of states to 325 cm^{-1} in the HV-derived approximate density of states (see Figs. 5 and 6 and Sec. IIIA).

As mentioned in Sec. I, x-ray[22] and infrared[22] measurements indicate that the AsS_3 pyramidal unit exists in both the amorphous and crystalline phase of As_2S_3. Taylor and Rubinstein[23] have placed an upper limit of ± 2° on the distribution in pyramidal apex angles in vitreous As_2S_3. We have attempted to determine whether that distribution of apex angles is alone sufficient to account for the continuous nature of the Raman spectrum. From the vibrational frequencies listed in Table III, the pyramidal bond-bending and bond-stretching force constants of the molecular model have been determined. Using those force constants and the valence force approximation we find that if the S-As-S bond angle is altered by ± 2° about a nominal value of 97.2°, then for a *symmetric* pyramidal AsS_3 molecule

$$\nu_1 = 344 \pm 4.4 \text{ cm}^{-1}\ , \quad \nu_2 = 162 \pm 2.2 \text{ cm}^{-1}\ ,$$

$$\nu_3 = 310 \pm 2.0 \text{ cm}^{-1}\ , \quad \nu_4 = 133 \pm 2.0 \text{ cm}^{-1}\ .$$

Thus, the distribution in apex angles produces only a slight broadening of the fundamental mode frequencies and can certainly not generate the continuous Raman spectrum observed experimentally. However, for a fixed apex angle of 97.2° a distribution of ± 9% in the radial force constant of the molecular model results for example in a ± 15-cm^{-1} spread in the ν_1-mode frequency. The cumulative effects of the distribution in both force constants and apex angles *can* account for the continuous nature of the Raman spectrum. Moreover, a ± 9% spread in force constants is by no means unrealistic. The As-S bond lengths in orpiment vary between inequivalent sites in the primitive cell by as much as 3%.[21] The variation in As-S bond lengths in vitreous As_2S_3 can be expected to be at least as large as if not larger. But, according to Gordy's rule[48] a 3% variation in As-S bond length results in a ≈ 5% variation in radial force constant. Gordy's rule is only an approximation[49]; a spread in radial force constant of ± 9% is therefore quite feasible.

We note with interest that as the AsS_3 pyramidal apex angle was increased from its nominal value of 97.2° the symmetric ν_1 mode decreased in frequency while the antisymmetric ν_3 mode increased in frequency. For apex angles greater than 108°, the ν_3 mode had a higher frequency than the ν_1 mode. Therefore, it is not surprising that the planar "pyramid" of the random-network model which has an apex angle of 120° should exhibit an antisymmetric mode of higher frequency than the symmetric mode in the region around 320 cm^{-1}.

Finally, the molecular model can be used to qualitatively explain the remarkable similarities in the approximate densities of states of vitreous and crystalline As_2S_3 shown in Fig. 9. Lucovsky and Martin[15] have pointed out that all of the major groups of eigenfrequencies in orpiment coincide with frequencies determined from the molecular model. By choosing a structural unit composed of several pyramids, i.e., a bigger molecule, one could in principle use the molecular model to obtain all of the vibrational modes and eigenfrequencies of crystalline As_2S_3. The Raman spectrum or

equivalently the approximate density of states of the amorphous phase can then be obtained by appropriately broadening the discrete Raman lines or peaks in the approximate density of states of the "large molecule" to account for the distribution in force constants and bond angles. For example, if the force-constant and bond-angle distributions are Gaussian, the approximate density of states of vitreous As_2S_3 shown in Fig. 9 could be obtained by replacing each peak in the approximate density of states of the crystal by a Gaussian line and summing the overlapping amplitudes. Ward has intuitively but quite successfully used this procedure to calculate the Raman spectrum of vitreous As_2S_3 from the spectrum of orpiment.[12]

V. CONCLUSION AND SUMMARY

The polarized Raman spectra of vitreous As_2S_3 have been studied as a function of temperature and compared with the spectra calculated from the planar-random-network model and the molecular model both of which give reasonable agreement with experiment. A new spectrum, the depolarization spectrum, has been defined for amorphous solids. Only the molecular model of vitreous As_2S_3 yields results in agreement with the observed depolarization spectrum. In addition, it is the depolarization spectrum, not the Raman spectrum, which determines the applicability of the Shuker–Gammon data-reduction technique to a given amorphous solid.

Inherent in the molecular model is the assumption of negligible intermolecular coupling. On the basis of that model, the depolarization ratio of antisymmetric vibrational modes is $\frac{3}{4}$. Yet the depolarization spectrum of vitreous As_2S_3 has a maximum amplitude of $\frac{1}{2}$ [50] (at $\approx 11\text{-cm}^{-1}$ Raman shift) (see Fig. 10). We believe that the failure of the depolarization spectrum to achieve the theoretical maximum amplitude of $\frac{3}{4}$ is a manifestation of intermolecular coupling. The coupled modes have admixtures of symmetric and antisymmetric eigenvectors of the AsS_3 unit.

Finally, it is possible to roughly characterize amorphous solids by their molecularity. Clearly vitreous As_2S_3 and As_2Se_3 are molecular since the molecular model works quite well for these materials. Amorphous Si is nonmolecular; for any chosen molecular structural unit of that substance the intermolecular coupling is just as strong as the intramolecular coupling. On the basis of the above discussion, amorphous Se and Te might best be described as quasimolecular.

Molecular amorphous solids and nonmolecular amorphous solids yield qualitatively quite similar Raman spectra which are continuous and exhibit broad peaks but no sharp structure. On the other hand, molecular and nonmolecular amorphous solids exhibit quite different depolarization spectra. For instance, the depolarization spectrum of tetrahedrally bonded amorphous Si has a *constant*[17] amplitude. Apparently, the more molecular the amorphous solid is, the more irregular is its depolarization spectrum. The depolarization spectra of amorphous Se and Te should be of considerable interest since these materials have a mixture of molecular and nonmolecular properties.

Note Added in Proof: Profitt and Porto have recently described a technique which can be used to automatically record depolarization spectra. See, W. Profitt and S. P. S. Porto, J. Opt. Soc. Am. 63, 77 (1973).

ACKNOWLEDGMENTS

Thanks are due to H. Fritzche for several valuable discussions and to S. A. Rice for familiarizing us with some of the details of Gordy's rule. Some of the samples of vitreous As_2S_3 used in this study were donated to us by John Wagner of the Servo Corp. of America.

---

†Work supported by the U.S. AEC under contract No. AT 11-1 (2126). General support of the Materials Research Laboratory of the University of Chicago by the NSF is acknowledged.

*Shell Foundation Fellow.

‡Submitted to the Department of Physics, The University of Chicago, in partial fulfillment of the requirements for the Ph.D. degree.

[1]M. H. Cohen, J. Non-Cryst. Solids **4**, 391 (1971).

[2]N. F. Mott and E. A. Davis, *Electronic Processes in Non-Crystalline Materials* (Clarendon, Oxford, England, 1970), p. 272.

[3]See, e.g., M. H. Brodsky, K. Weiser, and G. O. Pettit, Phys. Rev. B **1**, 2632 (1970); G. A. N. Connell and W. Paul, J. Non-Cryst. Solids **8**, 215 (1972).

[4]W. E. Spicer, T. M. Donovan, and J. E. Fischer, J. Non-Cryst. Solids **8**, 122 (1972).

[5]F. L. Galeener, in *Proceedings of the Eleventh International Conference on the Physics of Semiconductors* (Polish Scientific, Warsaw, 1972), p. 523.

[6]T. M. Donovan, E. J. Ashley, and W. E. Spicer, Phys. Lett. A **32**, 85 (1970).

[7]J. E. Fischer and T. M. Donovan, J. Non-Cryst. Solids **8**, 215 (1972).

[8]Servo Corp. of America, Hicksville, Long Island, N.Y.

[9]G. Getov, B. Kandilarov, P. Simidtchieva, and R. Andreytchin, Phys. Status Solidi **13**, K97 (1966); F. Kosek and J. Tauc, Czech. J. Phys. **20**, 94 (1970); J. Tauc, A. Menth, and D. L. Wood, Phys. Rev. Lett. **25**, 749 (1970).

[10]B. T. Kolomiets, T. F. Mazets, and Sh. M. Efendiev, J. Non-Cryst. Solids **4**, 45 (1970) (electrical and optical properties); Servo Corp. of American publication No. 2011, 1968 (unpublished) (thermal and optical properties); see, also, Ref. 9.

[11]R. J. Kobliska and S. A. Solin, Solid State Commun. **10**, 231 (1972).

[12]A. T. Ward, J. Phys. Chem. **72**, 4133 (1968).

[13]R. J. Kobliska and S. A. Solin, J. Non-Cryst. Solids **8**, 191

[14]G. Lucovsky, Phys. Rev. **6**, 1480 (1972).
[15]G. Lucovsky and R. M. Martin, J. Non-Cryst. Solids **8**, 185 (1971).
[16]V. Bermudez, J. Chem. Phys. **57**, 2793 (1972).
[17]J. E. Smith, Jr., M. H. Brodsky, B. L. Crowder, M. I. Nathan, and A. Pinczuk, Phys. Rev. Lett. **26**, 642 (1971).
[18]M. Wihl, M. Cardona, and J. Tauc, J. Non-Cryst. Solids **8**, 172 (1972).
[19]R. Zallen, M. L. Slade, and A. T. Ward, Phys. Rev. B **3**, 4257 (1971).
[20]J. P. Mathieu and H. Poulet, Bull. Soc. Fr. Mineral. Cristallogr. **93**, 532 (1970).
[21]N. Morimoto, Mineral. J. (Sapporo) **1**, 160 (1954).
[22]A. A. Vaipolin and C. A. Porai-Koshits, Fiz. Tverd. Tela **5**, 246 (1963) [Sov. Phys.-Solid State **5**, 178 (1963)]; Fiz. Tverd. Tela **5**, 256 (1963) [Sov. Phys.-Solid State **5**, 186 (1963)]; Fiz. Tverd. Tela **5**, 263 (1963) [Sov. Phys.-Solid State **5**, 479 (1963)]; P. C. Taylor, S. G. Bishop, and D. L. Mitchell, Phys. Rev. Lett. **27**, 414 (1971); S. V. Nemilov, Fiz. Tverd. Tela **11**, 1564 (1967) [Sov. Phys.-Solid State **6**, 1075 (1964)].
[23]Mark Rubenstein and P. C. Taylor, Phys. Rev. Lett. **29**, 119 (1972).
[24]Spectra Physics Model No. 125 He-Ne laser and Model No. 70 dye laser manufactured by the Spectra Physics Corp., Mountain View, Calif. We acknowledge the loan of the dye laser for test and evaluation.
[25]CRL Model No 52G, manufactured by Coherent Radiation Laboratories, Palo Alto, Calif.
[26]Manufactured by Jarrel-Ash Division, Fisher Scientific, Waltham, Mass.
[27]Manufactured by Electron Tube Division, ITT Corp., Fort Wayne, Ind.
[28]Manufactured by Andonian Assoicates, Waltham, Mass.
[29]A. F. Wells, *Structural Inorganic Chemistry*, 3rd ed. (Oxford U. P., London, 1962), p. 682; A. G. Fisher and A. S. Mason, J. Opt. Soc. Am. **52**, 721 (1962).
[30]S. A. Keneman, Appl. Phys. Lett. **19**, 205 (1971).
[31]S. A. Solin and A. K. Ramdas, Phys. Rev. B **1**, 1687 (1970); see, also, Ref. 11.
[32]Manufactured by the Perkin Elmer Corp., Norwalk, Conn.
[33]H. A. Szymanski, *Theory and Practice of Infrared Spectroscopy* (Plenum, New York, 1964), p. 76.
[34]R. Shuker and R. W. Gammon, Phys. Rev. Lett. **25**, 222 (1970).
[35]R. Louden, Adv. Phys. **13**, 423 (1964).
[36]For details of the computer smoothing routine see S. A. Solin, Ph.D. thesis (Purdue University, 1970) (unpublished).
[37]P. Flubacher, A. J. Leadbetter, J. A. Morrison, and B. P. Stoicheff, J. Phys. Chem. Solids **12**, 53 (1969).
[38]D. Weaire and R. Alben, Bull. Am. Phys. Soc. 18, 306 (1973).
[39]Since the scattered radiation was unanalyzed, the correction for instrumental transfer function was not included in the data of Fig. 9.
[40]T. R. Gilson and P. J. Hendra, *Laser Raman Spectroscopy* (Wiley, New York, 1970).
[41]E. B. Wilson, J. C. Decius, and P. C. Cross, *Molecular Vibrations* (McGraw-Hill, New York, 1955).
[42]We have neglected here first-order Raman scattering from coupled-mode excitations such as plasmons, polaritons, etc.
[43]Before the advent of laser sources, depolarization ratios were measured for the Raman lines of oriented single crystals as well as for gases and liquids.
[44]G. Herzberg, *Infrared and Raman Spectra of Polyatomic Molecules* (Van Nostrand, New York, 1945).
[45]L. B. Zlatkin and Ye. F. Markov, Phys. Status Solidi A **4**, 391 (1971).
[46]Infrared absorption from the bent chain "water-molecule" vibrations has been observed in As_2Se_3, a material which is isomorphic to As_2S_3 in the crystalline form and quite similar to it in the amorphous form; see Ref. 14.
[47]D. M. Hwang and S. A. Solin, Phys. Rev. B 7, 843 (1972).
[48]W. Gordy, J. Chem. Phys. **14**, 305 (1946).
[49]The error in the radial force constant of $AsCl_3$ calculated from Gordy's rule is 15%. See Ref. 48.
[50]The discrepancy between the theoretical value of 3/4 for ρ and the observed value of 1/2 is not an experimental artifact. When measured using a large collection aperture ($\sim$f1.2 in our case) for the Raman scattered radiation, the observed depolarization ratio is *larger*, not smaller, than the true depolarization ratio. See Ref. 40, p. 76.

PHYSICAL REVIEW B VOLUME 8, NUMBER 2 15 JULY 1973

Infrared Reflectivity of Paratellurite, TeO_2†

D. M. Korn,* A. S. Pine, G. Dresselhaus, and T. B. Reed
Lincoln Laboratory, Massachusetts Institute of Technology, Lexington, Massachusetts 02173
(Recieved 14 February 1973)

The polar-phonon spectrum of paratellurite has been obtained from polarized infrared reflectivity at 295 and 85 °K. The eight E and four A_2 modes are identified; the mode frequencies, oscillator strengths, and dampings are determined from a dispersion analysis of the data. The anisotropic frequencies of the coupled A_2 and E modes for oblique phonons in the extraordinary ray are also presented.

The polar-phonon spectrum of paratellurite has been obtained from the polarized infrared reflectivity at 295 and 85 °K. Paratellurite is a tetragonal, D_4^4, form of TeO_2 with four formula units in the elementary cell.[1] The zone-center optical phonons have the symmetries $4A_1+4A_2(z)+5B_1+4B_2+8E(x,y)$, of which the infrared-active branches are labeled with their polarizations where z is parallel to the crystal c axis. All of these lattice-mode symmetries are Raman active except for the pure $A_2(z)$ phonons. In this paper the eight E and four A_2 modes are identified; and the mode frequencies, oscillator strengths, and dampings are determined from a dispersion analysis of the